ACS APPLIED MATERIALS & INTERFACES

Research Article

www.acsami.org

CO_2 Adsorption on Amine-Functionalized Periodic Mesoporous Benzenesilicas

Kyohyun Sim,[†,§] Nakwon Lee,[†,§] Joonseok Kim,[†] Eun-Bum Cho,*[,†] Chamila Gunathilake,[‡] and Mietek Jaroniec*[,‡]

[†]Department of Fine Chemistry, Seoul National University of Science and Technology, Seoul 139-743, Korea

[‡]Department of Chemistry and Biochemistry, Kent State University, Kent, Ohio 44242, United States

Supporting Information

ABSTRACT: CO_2 adsorption was investigated on amine-functionalized mesoporous silica (SBA-15) and periodic mesoporous organosilica (PMO) samples. Hexagonally (*p6mm*) ordered mesoporous SBA-15 and benzene-PMO (BPMO) samples were prepared in the presence of Pluronic P123 block copolymer template under acidic conditions. Three kinds of amine-containing organosilanes and polyethylenimine were used to functionalize SBA-15 and BPMO. Small-angle X-ray scattering and nitrogen adsorption isotherms showed that these samples featured ordered mesostructure, high surface area, and narrow pore size distributions. Solid-state ^{13}C- and ^{29}Si cross-polarization magic-angle spinning NMR spectra showed chemical linkage between amine-containing modifiers and the surface of mesoporous materials. The chemically linked amine-containing modifiers were found to be on both the inner and outer surfaces. *N*-[3-(trimethoxysilyl)propyl]-ethylenediamine-modified BPMO (A2-BPMO) sample exhibited the highest CO_2 uptake (i.e., ~3.03 mmol/g measured on a volumetric adsorption analyzer) and the fastest adsorption rate (i.e., ~13 min to attain 90% of the maximum amount) among all the samples studied. Selectivity and reproducibility measurements for the A2-BPMO sample showed quite good performance in flowing N_2 gas at 40 mL/min and CO_2 gas of 60 mL/min at 25 °C.

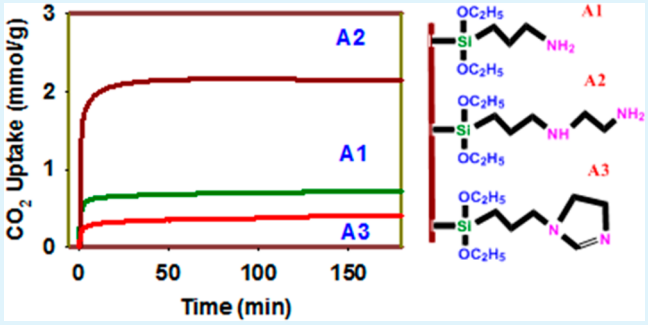

KEYWORDS: *CO_2 adsorption, periodic mesoporous organosilica, polyethylenimine, N-[3-(trimethoxysilyl)propyl]ethylenediamine*

INTRODUCTION

As compared to the last 20 000 years a significant change in the global climate occurred as a consequence of human activities such as extensive burning fossil fuels and deforesting the earth. It was shown that the annual emission of CO_2 has increased by ~80% between 1970 and 2004, and the current atmospheric CO_2 concentration exceeds by ~25% the level of 300 ppm observed in past before 1950.[1] Nowadays, the reduction of CO_2 emission became the key issue to slow down the global warming. Recently, various adsorption techniques and materials for CO_2 capture have been developed such as zeolitic molecular sieves,[2] oxides,[3] metal−organic frameworks,[4] activated carbons,[5] and amine-containing materials.[6−9] For decades the amine-containing materials such as liquid amines[10] have been used in industrial processes to capture CO_2. Extensive efforts have been made toward using aqueous alkanolamines such as monoethanolamine (MEA), diethanolamine (DEA), diglycolamine, and triethanolamine (TEA) for CO_2 capture.[11] It was reported that these species are able to attach CO_2 via reversible formation of carbamate, carbonate, and bicarbonate species.[11] In this process, amine solutions mixed with ionic liquids chemically absorb ~3−4 mmol of CO_2 per gram of amine, and reversibly release captured CO_2 by heating mixture above 100 °C.[12] Nevertheless, this process possesses several disadvantages, including high cost and high energy consumption associated with evaporation of CO_2. Furthermore, the effectiveness of this process is affected by oxidative degradation of amine, their low stability, and by interference of impure gases such as SO_2, NO_2, and NO.[13,14] As a result, the research on the CO_2 capture is gradually shifting from liquid amine-based scrubbing to solid adsorption to overcome the drawbacks of the former.[15]

Mesoporous silica is a very popular solid adsorbent for gas- and liquid-phase applications including CO_2 sorption. Recently, porous solid adsorbents such as silica have been modified by the aforementioned amine-containing compounds[16] to increase their affinity toward CO_2. This modification is usually performed by impregnation of amines[16−25] or by grafting amine-functional groups on the pore walls.[26,27,31] Studies of polyethylenimine (PEI)-loaded MCM-41 mesoporous silica sorbents showed a substantial increase in the CO_2 adsorption capacity for the sample with 75 wt% PEI loading under pure CO_2 gas conditions.[17,18] Sayari et al. investigated the effect on the pore

Received: January 11, 2015
Accepted: March 5, 2015
Published: March 5, 2015

DOI: 10.1021/acsami.5b00306
ACS Appl. Mater. Interfaces 2015, 7, 6792−6802

Table 1. Physicochemical Parameters Determined from N_2 Sorption Isotherms and Small-Angle X-ray Scattering[a]

sample	V_{sp} (cc/g)	V_{mic} (cc/g)	S_{BET} (m^2/g)	W_{max} (nm)	V_t (cc/g)	d_{sp} (nm)	a (nm)	t (nm)
SBA-15	0.65	0.04	443	8.3	0.68	10.17	11.74	3.4
A2-SBA-15	0.33	0.01	190	7.2	0.37	10.23	11.81	4.6
PEI/SBA-15	0.34	0.01	195	7.0	0.39	10.05	11.60	4.6
PEI/A2-SBA-15	0.20	0.01	24	2.7	0.21	10.30	11.89	9.2
BPMO	0.90	0.10	645	8.7	0.96	10.30	11.89	3.2
A2-BPMO	0.32	0.01	180	7.2	0.37	10.05	11.60	4.4
PEI/BPMO	0.28	0.01	167	7.6	0.33	10.10	11.66	4.1
PEI/A2-BPMO	0.18	<0.01	39	2.3	0.18	10.97	12.67	10.4

[a]Notation: V_{sp} = single point pore volume calculated at $P/P_0 = 0.98$; S_{BET} = specific surface area calculated from adsorption data in relative pressure range of 0.05−0.20; W_{max} = pore width calculated at the maximum of PSD using improved KJS method; V_t = total pore volume calculated by integration of the PSD curve; d_{sp} = Bragg's d-spacing ($= 2\pi/q^*$, q^* is the q-value at the maximum of (100) peak for hexagonal *p6mm* structure; a = unit cell parameter ($= 2d_{100}/\sqrt{3}$ for *p6mm*); t = pore wall thickness ($= a - W_{max}$ for *p6mm*).

size and pore volume via impregnation of diamine[19] and triamine[20] into pore-expanded MCM-41. Analogous studies have been carried out for different types of mesoporous silica materials such as SBA-12, SBA-15, SBA-16, KIT-6, and HMS.[21−23] Impregnation of porous adsorbents with amines has several advantages including simple manufacturing, low cost, and ability of loading many amines. However, the impregnated materials often did not feature a significant enhancement in the CO_2 sorption due to the pore blocking, which resulted in reducing the pore volume and specific surface area of the resulting sorbents.[24] In addition, physisorption of aminosilanes was shown to be instable, which in consequence reduced the amine loading after several adsorption−desorption cycles and shortened the lifetime of impregnated adsorbents.[25] Meanwhile, the grafting of silica with aminosilanes has been suggested to solve the aforementioned drawbacks of impregnated sorbents. The amine-grafted sorbents showed similar adsorption characteristics to amine-impregnated materials such as good selectivity, fast adsorption and desorption rates, and low energy consumption.[27] For instance, a significant improvement in the CO_2 uptake has been reported for mesoporous silica modified with 3-aminopropyl triethoxysilane (APTES) and *N*-[3-(trimethoxysilyl)propyl]ethylenediamine (TSPED).[28,29]

Recently, it was shown that hydrophobic sites on the sorbents' surfaces have a positive effect on CO_2 uptake. Sayari et al. observed that the rate of CO_2 sorption was considerably faster after coating long alkyl chains on the pore walls of the pore-expanded MCM-41. It was shown that the surface layer of hydrophobic alkyl chains improved dispersion of PEI.[30] Periodic mesoporous organosilica (PMO) was also investigated to confirm the effect of hydrophobic groups inside the pore framework. PMO is an interesting type of hybrid material featuring organic moieties in siliceous framework; it can be synthesized by condensation of organosilica precursors with organic bridging groups such as ethane, thiophene, benzene, biphenyl, and so on.[31,32] There is one report on the ethylene-bridged PMO with grafted amine groups; this material showed high CO_2 affinity depending on the nitrogen content inside amines.[33]

Stimulated by the above study, here we investigate the interplay between the loading and structure of nitrogen-containing ligands and the hydrophobicity of the porous supports used for amine grafting. Namely, in this work we used an effective procedure for the preparation of amine-grafted SBA-15 and benzene-bridged PMO (BPMO) adsorbents for CO_2 uptake. APTES, TSPED, and triethoxy-3-(2-imidazolin-1-yl)-propylsilane (TEIPS) were employed to decorate the pore walls of SBA-15 and BPMO materials with A1, A2, and A3 amine groups, respectively. Three types of amine groups (A1, A2, and A3) were explored in this study because their diverse chemical structures show different affinity toward CO_2 molecules. The aforementioned design of adsorbents allowed us to show the dependence of the CO_2 uptake on various factors such as the structure and reactivity of amine groups, the availability of N lone pair for interaction with CO_2, and the steric hindrance caused by the branched structure of N-containing ligands. To increase the content of nitrogen the resulting amine-functionalized SBA-15 and BPMO materials were also subjected to the post-synthesis modification by using PEI polymer and amine-containing organosilanes. The samples studied were thoroughly characterized by adsorption, thermogravimetry, elemental analysis, and solid-state NMR. For instance, the solid-state ^{29}Si NMR analysis showed the chemical linkage between amine-containing modifiers and mesoporous silica surface. Finally, the CO_2 equilibrium and kinetic adsorption isotherms were measured by using 'volumetric adsorption and thermogravimetric analyzers, respectively, and analyzed to determine the effect of benzene-bridging groups, the structure of aminosilanes, and the PEI loading on the CO_2 uptake. Also, the selectivity and reproducibility of an amine-functionalized benzene-PMO in flowing mixed gas were studied.

EXPERIMENTAL SECTION

Materials. A commercial Pluronic P123 ($EO_{20}PO_{70}EO_{20}$) triblock copolymer was used as a soft template. Tetraethylorthosilicate (TEOS) and 1,4-bis(triethoxysilyl)benzene (BTEB) were used as silica and organosilica precursors. Three kinds of amine-containing functional reagents such as APTES, TSPED, and TEIPS were used to functionalize the pore walls of SBA-15 and BPMO materials with A1, A2, and A3 amine groups, respectively. Branched polyethylenimine with an average molecular weight M_n of ∼10 000 g/mol (GPC; PEI) and triethoxyphenylsilane (TEPS) were also used to modify two mesoporous siliceous supports. All chemicals were obtained from Sigma-Aldrich and used as purchased.

Synthesis of Mesoporous Silica and Organosilica Materials. SBA-15 was synthesized in the presence of P123 triblock copolymer. P123 (2.5 g) and 15.0 g of hydrochloric acid (37%) were dissolved in 75 mL of distilled water, and the mixture was stirred with magnetic bar in a glass bottle of 125 mL at 30 °C. After stirring for 2 h, 5.2 g of TEOS was added, and the mixture was stirred for further 20 h at 30 °C followed by aging for 24 h at 100 °C. To remove the block copolymer template and unreacted species, a mixture of 56 mL of ethanol and 4 mL of hydrochloric acid was used as a washing solvent under magnetic stirring for 24 h at 78 °C. The final SBA-15 samples were obtained after filtration using suction flask. An analogous route was used for the synthesis of periodic mesoporous organosilica with benzene-bridging group

DOI: 10.1021/acsami.5b00306
ACS Appl. Mater. Interfaces 2015, 7, 6792−6802

(BPMO). P123 (2.97 g) and 0.6 g of hydrochloric acid were dissolved in 108 mL of distilled water. The mixture was stirred for 2 h in a glass bottle of 125 mL at 40 °C, and 3.03 g of BTEB was added into the mixture. After further stirring for 20 h, the precipitates were aged for 24 h at 100 °C. Final BPMO samples were obtained by washing with acidic solvent and filtering using suction flask.

Amine and Phenylene Functionalization. APTES (A1), TSPED (A2), and TEIPS (A3) were used to functionalize the surface of SBA-15 and BPMO materials. Before using amine-containing organosilane precursors, SBA-15 and BPMO materials were kept in vacuum oven for 1 d. In a typical preparation, 1 g of mesoporous material, 0.6 mL of amine-containing organosilane precursor, and 50 mL of toluene as a solvent were mixed in a glass bottle of 125 mL. The mixture was stirred magnetically in oil bath at 110 °C for 8 h. The final product was collected after filtering using a suction flask with ethanol and acetone. Analogous step was taken to functionalize the surface using phenylene-containing TEPS organosilane precursor. The main amine-grafted sample names are A2-SBA-15 and A2-BPMO obtained by using TSPED (A2), as listed in Table 1.

Preparation of Polyethyleneimine–Mesoporous Silica Composites. Branched PEI was used to prepare the PEI-modified mesoporous silica-based composites. Before using PEI polymer, SBA-15, BPMO, and amine-modified samples were kept in a vacuum oven for 1 d. In a typical preparation, 1 g of mesoporous material, 0.4 g of PEI, and 10 g of methanol solvent were stirred at 25 °C for 1 d in a glass bottle of 125 mL. The final composites were obtained after treatment in vacuum oven at 80 °C for 1 d. The main PEI-modified sample names are PEI/SBA-15, PEI/A2-SBA-15, PEI/BPMO, and PEI/A2-BPMO obtained by using PEI polymer, as listed in Table 1.

Measurements and Calculations. The small-angle X-ray scattering (SAXS) experiments were performed using synchrotron radiation source (E = 10.5199 keV, λ = 1.1785 Å) of a 3C beamline in Pohang Accelerator Laboratory (PAL). Each sample was placed in a copper-alloy multisample holder and secured on both sides using a Kapton tape.

Nitrogen adsorption–desorption isotherms were measured at −196 °C on a Micromeritics 2010 analyzer. The samples were degassed at 110 °C under vacuum for at least 2 h before each measurement. The Brunauer–Emmet–Teller (BET) specific surface area was calculated from adsorption data in the relative pressure (P/P_0) range from 0.05 to 0.20. The single-point pore volume was evaluated from the amount adsorbed at the relative pressure of 0.98. The pore size distributions (PSD) were calculated from adsorption branches of the isotherms by using the improved Kruk–Jaroniec–Sayari (KJS) method.[34] The total pore volume was calculated by integration of the PSD. The pore wall thickness (t) was estimated from the pore size (W_{max}) obtained at the maximum of PSD and the unit cell parameter (a) obtained by SAXS (i.e., $t = a - W_{max}$).

The solid-state ^{13}C and ^{29}Si cross-polarization magic-angle spinning (CP-MAS) NMR spectra were obtained with a Bruker AVANCE II$^+$ (400 MHz) spectrometer using a 4 mm MAS probe at the KBSI Seoul Western Center. Experimental conditions for ^{13}C CP-MAS NMR spectra were as follows: 10 kHz of spinning rate, 3 s of delay time, 100.62 MHz of Lamor frequency, and 2 ms of contact time. ^{29}Si CP-MAS NMR spectra were obtained from the following experimental conditions: 6 kHz of spinning rate, 3 s of delay time, and 79.488 MHz of radio frequency. The chemical shifts were obtained with respect to the tetramethylsilane reference peak.

The quantitative analysis of nitrogen content in the amine-modified samples was performed using a Flash EA 1112 series (CE Instruments) at the KBSI Seoul Center.

Thermogravimetric Analysis for CO_2 Adsorption. CO_2 gas uptake was measured using a microbalance inside Q50 thermogravimetric analyzer (TA Instruments). Before measuring the gas uptake using a Q50 analyzer, samples were kept in vacuum oven for 1 d. Approximately 10 mg of the modified mesoporous samples was loaded in the sample plate and sealed in the cylindrical chamber. As a first step, the cylindrical chamber was purged at 110 °C for 2 h in flowing nitrogen gas of 100 mL/min. Gas uptake was recorded for 3 h in flowing CO_2 gas of 100 mL/min after cooling to 25 °C under a nitrogen flow. Selective uptake was measured using A2-grafted BPMO (A2-BPMO) sample in flowing nitrogen gas of 40 mL/min and carbon dioxide gas of 60 mL/min at 25, 80, and 100 °C. Reproducibility for CO_2 adsorption was measured repeatedly without changing sample in a closed cylindrical chamber using A2-BPMO sample. Reproducibility was obtained up to nine times in flowing nitrogen gas of 40 mL/min and carbon dioxide gas of 60 mL/min at 25 °C.

CO_2 Adsorption Measurements on Volumetric Adsorption Analyzer. CO_2 sorption was measured on the samples (amine, phenylene, and PEI–mesoporous silica) studied in the pressure range up to 1.2 atm using ASAP 2020 (Micromeritics, Inc., GA) volumetric adsorption analyzer at 25 °C and ultrahigh purity (99.99%) CO_2. Prior to analysis, all samples were outgassed at 110 °C for 2 h under vacuum.

RESULTS AND DISCUSSION

Amine-grafted SBA-15 and BPMO samples were prepared by a co-condensation method in the presence of a P123 block copolymer template. Additionally, amine-grafted mesoporous samples as well as pure SBA-15 and BPMO were modified by mixing them with amine-containing PEI polymer. Among amine-containing organosilica precursors used in this study, incorporation of TSPED into mesoporous silica showed the best performance for CO_2 sorption. Therefore, the characterization and additional measurement were conducted mainly with A2- and PEI-modified samples, as listed in Table 1.

Synchrotron SAXS patterns for representative eight samples are shown in Figure 1. All the samples show highly ordered

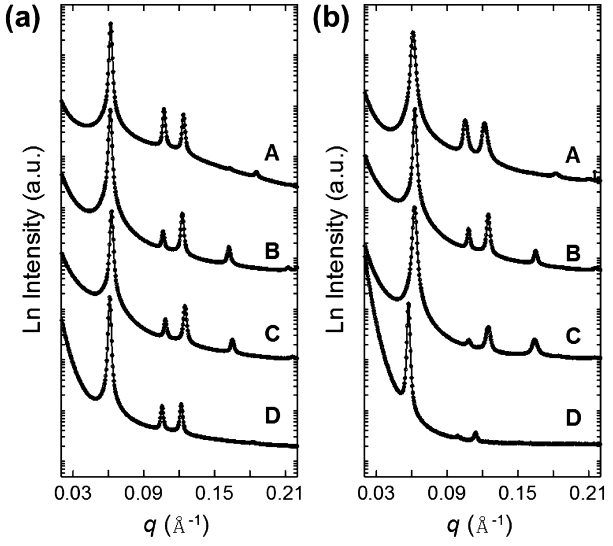

Figure 1. Synchrotron SAXS patterns recorded for (a) hexagonal (*p6mm*) SBA-15-based and (b) benzene–PMO-based mesoporous materials prepared under acidic conditions. The sequence of the SAXS patterns from (a) to (b) refer to the following samples: (a-A) SBA-15, (a-B) A2-SBA-15, (a-C) PEI/SBA-15, (a-D) PEI/A2-SBA-15, (b-A) BPMO, (b-B) A2-BPMO, (b-C) PEI/BPMO, and (b-D) PEI/A2-BPMO.

hexagonal (*p6mm*) mesostructure with 2–4 peaks on the SAXS patterns. The unit cell parameters (a) for SBA-15-based samples are determined in the range of 11.60–11.89 nm. Those for BPMO-based samples are in the range of 11.60–12.67 nm. Both PEI- and amine-modified samples (e.g., PEI/A2-SBA-15 and PEI/A2-BPMO) show enlarged unit cell parameters, and the BPMO-based sample shows larger unit cell parameter by 0.78 nm as compared to that of pure BPMO, which indicates easier incorporation of PEI into the mesopores of amine-grafted PMO sample than pure PMO and modified-SBA-15.

DOI: 10.1021/acsami.5b00306
ACS Appl. Mater. Interfaces 2015, 7, 6792–6802

As shown in Figures 2 and 3 (left) nitrogen adsorption−desorption isotherms are type IV except those for PEI/A2-SBA-15 and PEI/A2-BPMO. All isotherms except for the aforementioned two samples show distinct hysteresis indicating a significant nitrogen uptake in the range of 0.5−0.75 P/P_0. The BET specific surface area is significantly reduced after modification with amine and PEI from 645 to 39 m^2/g, and the pore volume is also reduced from 0.90 to 0.18 cc/g, which is shown in Table 1. The micropore volumes for pure SBA-15 and BPMO samples were determined as 0.04 and 0.10 cc/g, respectively. Note that the modified samples showed very small micropore volumes below 0.01 cc/g. The maximum pore widths for SBA-15- and BPMO-based samples, obtained by improved KJS method, were in the range of 2.7−8.3 nm and 2.3−8.7 nm, respectively, as listed in Table 1. Modified samples showed smaller pore widths than those of pure samples. Figures 2 and 3 (right) clearly show that the pore size distributions are very narrow. Also, the pore wall thickness was calculated using unit cell parameter and pore width. The largest wall thickness was calculated up to 10.4 nm for PEI/A2-BPMO sample, which is attributed to the modification of amine groups on inner surfaces. As shown in Table 1, the nitrogen adsorption results clearly indicate that the amine-functionalization was successfully achieved on the inner surfaces as well as the outer surfaces of mesoporous materials.

To confirm the presence of amine groups in the mesoporous samples, solid-state ^{13}C- and ^{29}Si NMR spectra were recorded. Figure 4 shows solid-state ^{13}C CP-MAS NMR spectra of the A2-SBA-15, PEI/SBA-15, A2-BPMO, and PEI/BPMO samples,

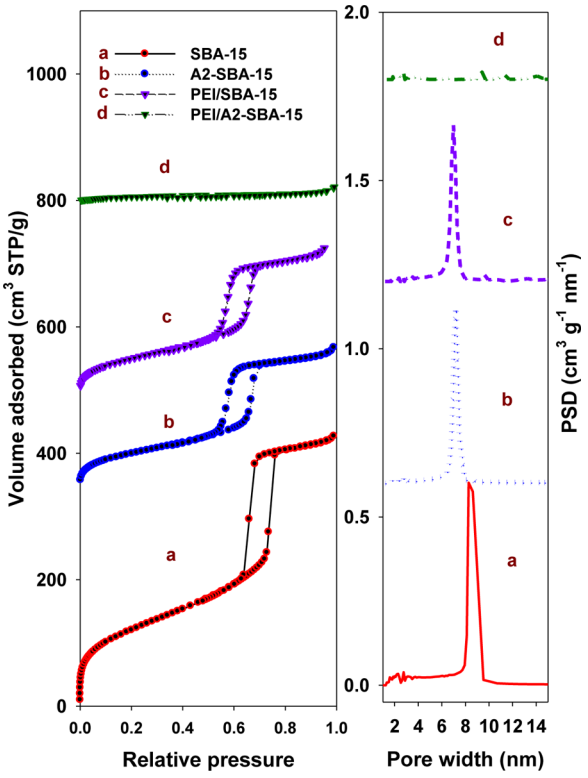

Figure 2. Nitrogen adsorption isotherms (left) and the PSD curves (right) for SBA-15-based mesoporous materials; A2-SBA-15 (b), PEI/SBA-15 (c), and PEI/A2-SBA-15 (d) isotherms are shifted by 300, 500, and 700 cm^3 STP/g, respectively, from that on SBA-15 (a). PSD curves are shifted by multiple of 0.6 $cm^3\ g^{-1}\ nm^{-1}$.

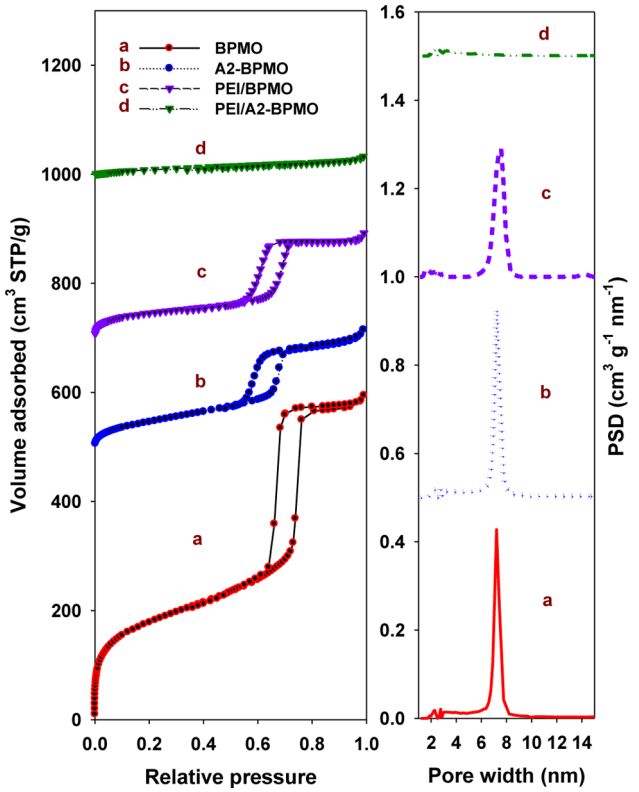

Figure 3. Nitrogen adsorption isotherms (left) and the PSD curves (right) for BPMO-based mesoporous materials; A2-BPMO (b), PEI/BPMO (c), and PEI/A2-BPMO (d) isotherms are shifted by 300, 500, and 700 cm^3 STP/g, respectively, from that on BPMO (a). PSD curves are shifted by multiple of 0.6 $cm^3\ g^{-1}\ nm^{-1}$.

respectively. Numbers inside the schemes in upper part of Figure 4 represent the chemical shifts (ppm) for respective carbons in amine-containing molecules, which were simulated by ChemDraw software package. Blue dotted lines indicate the chemical shifts (ppm) for carbons in amine-containing organosilica (TSPED), and red dotted lines are for PEI. Asterisks refer to the spinning side bands of cyclic phenylene group in BPMO-based samples. Dots refer to the residual polymer templates.

TSPED-containing SBA-15 (Figure 4a) and BPMO (Figure 4c) samples show clearly four resonance peaks at ∼11, 24, 39, and 51 ppm similar to the simulated values of 7.3, 25.8, 41.1, and 51.6−52.8 ppm. PEI-containing SBA-15 (Figure 4b) and BPMO (Figure 4d) samples show two overlapped resonance peaks at 38−39 and 48−52 ppm, which are also similar to the simulated values of 38.9−41.4 and 46.9−55.7 ppm. A sharp resonance peak at 133 ppm in Figure 4 (spectra c and d) represents phenylene groups originated from BTEB organosilane precursor. Therefore, the ^{13}C NMR spectra in Figure 4 clearly show that the hydrocarbon alkyl groups inside amine-containing materials as well as phenylene bridging group inside BPMO exist in functionalized mesoporous materials without any bond cleavage.

Figure 5a presents solid-state ^{29}Si CP-MAS NMR spectra of SBA-15 (A), A2-SBA-15 (B), and PEI/SBA-15 samples (C). Figure 5a (spectrum A) shows typical resonances (i.e., Q peaks) of SBA-15 sample at −91, −101, and −110 ppm, which are indexed as Q^2 ($(HO)_2$-Si-$(OSi)_2$), Q^3 ((HO)-Si-$(OSi)_3$), and Q^4 (Si-$(OSi)_4$), respectively. These structures are formed mainly due to the hydrolysis of TEOS and aminosilane followed by condensation reactions.

DOI: 10.1021/acsami.5b00306
ACS Appl. Mater. Interfaces 2015, 7, 6792−6802

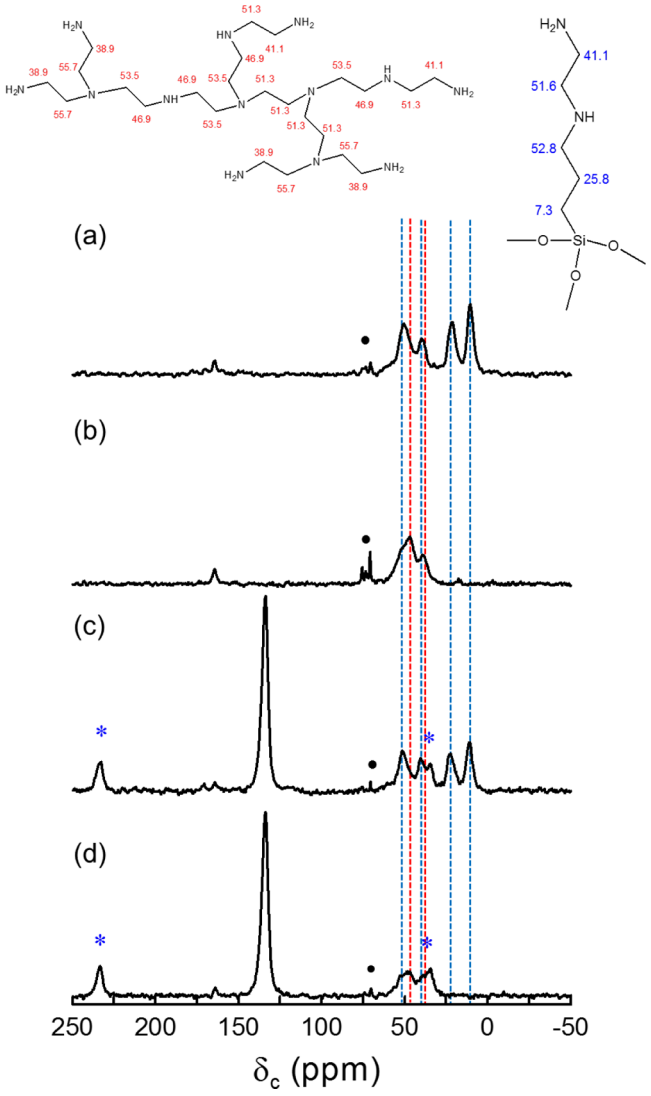

Figure 4. Solid-state ^{13}C CP-MAS NMR spectra for A2-SBA-15 (a), PEI/SBA-15 (b), A2-BPMO (c), and PEI/BPMO (d) mesoporous silica samples. Numbers inside the schemes represent the chemical shifts (ppm) for respective carbons simulated by ChemDraw software package. Blue dotted lines are for carbons in an amine-containing organosilica, and red dotted lines are carbons in PEI. Asterisks refer to the spinning side bands of cyclic phenylene group in BPMO-based samples. Dots refer to the residual polymer templates.

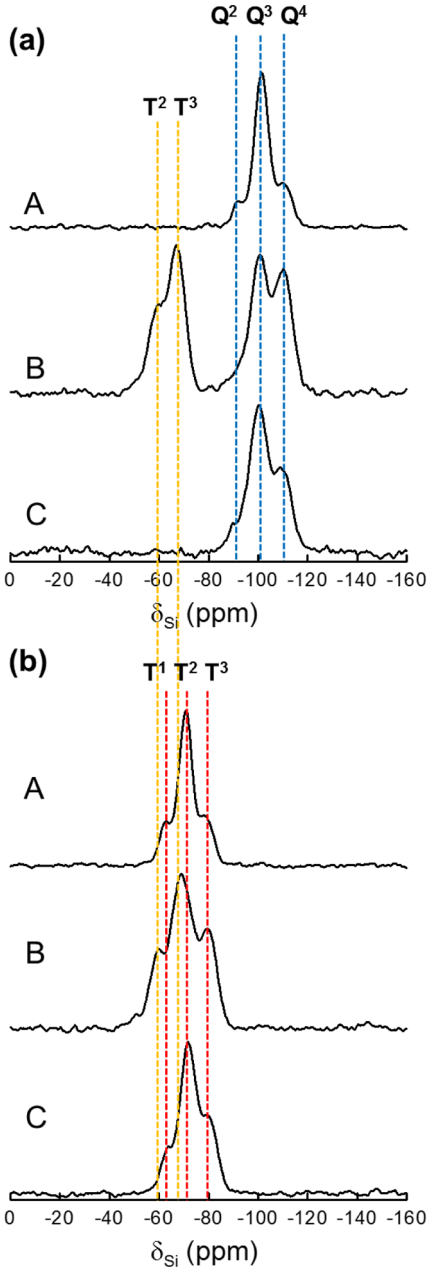

Figure 5. Solid-state ^{29}Si CP-MAS NMR spectra of (a-A) SBA-15, (a-B) A2-SBA-15, (a-C) PEI/SBA-15, (b-A) BPMO, (b-B) A2-BPMO, and (b-C) PEI/BPMO mesoporous silica samples.

Figure 5a (spectrum B) shows T peaks in addition to the typical Q peaks. The resonances for T peaks located at −59.5 and −68 ppm can be indexed as T^2 (C-Si-$(OSi)_2(OH)$) and T^3 (C-Si-$(OSi)_3$) and originate from TSPED (A2 group) organosilane precursor.[35] Note that Q^2 peak of A2-SBA-15 (Figure 5a, spectrum B) is negligible and the Q^4/Q^3 peak ratio is higher as compared to Q^4/Q^3 of pure SBA-15 (Figure 5a, spectrum A), which strongly suggests the formation of new chemical bonds between the hydroxyl group on the surface of SBA-15 and the hydrolyzed methoxy groups inside TSPED organosilane additive. Figure 5a (spectrum C) shows only Q resonances but shifted slightly as −90, −100, and −109 ppm as compared to those of SBA-15 (Figure 5a, spectrum A). As in the previous case, Q^2 is negligible and the Q^4/Q^3 peak ratio is larger as compared to that of pure SBA-15. Similarly as in the amine-functionalized A2-SBA-15 sample, new chemical bonds between the hydroxyl group on the surface of SBA-15 and the amine groups inside PEI polymer chains are formed.

Figure 5b shows ^{29}Si CP-MAS NMR spectra of BPMO (A), A2-BPMO (B), and PEI/BPMO (C) samples. Figure 5b (spectrum A) shows typical resonances (i.e., T peaks) of BPMO sample at −62, −71, and −80 ppm, which are indexed as T^1 (C-Si-$(OSi)(OH)_2$), T^2 (C-Si-$(OSi)_2$ (OH)), and T^3 (C-Si-$(OSi)_3$) chemical linkages cross-linked between BTEB organosilane precursors, respectively. Figure 5b (spectrum B) shows shifted T^1 and T^2 peaks at −60 and −69 ppm as well as a static T^3 peak at −80 ppm. Considering that T peaks appear in the spectrum of A2-SBA-15 (Figure 5a, spectrum B), it seems that T^1 and T^2 peaks overlap with those of siloxane bonds attributed to an additional TSPED (A2) organosilane precursor. It can be noted that the T^3/T^2 peak ratio of A2-BPMO (Figure 5b,

DOI: 10.1021/acsami.5b00306
ACS Appl. Mater. Interfaces 2015, 7, 6792−6802

spectrum B) is higher as compared to that of pure BPMO (Figure 5b, spectrum A), which strongly suggests the formation of new chemical bonds between the hydroxyl group on the surface of BPMO and the hydrolyzed methoxy groups inside TSPED organosilane additive. Figure 5b (spectrum C) shows only T resonances, and the T^3/T^2 peak ratio is higher as compared to that of pure BPMO (Figure 5b, spectrum A). It is also suggested that new chemical bonds between the hydroxyl group on the surface of BPMO and the amine groups inside PEI polymer chains are formed.

To investigate the relationship between amine-grafted mesoporous organosilica samples and CO_2 adsorption, three kinds of amine-containing organosilane additives were selected as shown in Figure 6a. Generally, acidic CO_2 gas molecules have

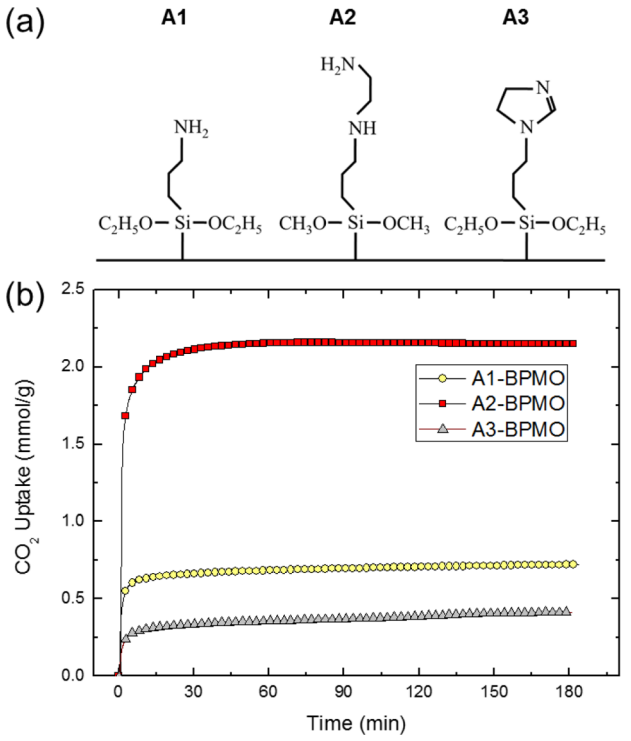

Figure 6. Schematic illustration of chemical fixation of three kinds of amine-containing organosilica precursors (a) and the comparative CO_2 adsorption kinetics for respective amine-functionalized BPMO materials (b).

tendency to form zwitterions due to the acid–base interactions with amine functional groups.[36] This CO_2 reactivity enhanced the CO_2 uptake of the adsorbents studied. The primary amine group is known to show the highest reaction rate toward CO_2, while the reaction rate in the case of secondary amine groups is lower and in the case of tertiary amines is even lower in accordance to the number of protons combined with nitrogen.[37] Among three ligands used A1 is the primary amine group and easily accessible for interaction of CO_2 with N lone pair, but the suitable distribution of these groups is essential for effective CO_2 binding (see below). A2 contains both primary and secondary amine groups in the ligand, and the lone pairs in both N atoms are available for interaction with CO_2.

The overall reaction between CO_2 and the primary and secondary amines occurs via carbamate formation, which requires the presence of two neighboring groups as it was shown by Hiyoshi et al. and Prasetyanto et al.[38,39] According to the Dankwerts' mechanism,[40] CO_2 effectively binds two neighboring amine groups, while this interaction is weaker with isolated amine groups. Thus, primary amine groups (A1) satisfy the aforementioned condition when they are close to each other. However, in the case of A2, both –NH and $-NH_2$ are available for effective binding with CO_2 molecule because they are present in a single A2 group, which makes it more prone for efficient CO_2 binding as compared to A1. The third ligand studied, A3, has also two N atoms in a single ring, which both are tertiary amines. However, these nitrogen atoms show sp^2 and sp^3 hybridizations, respectively; note that the lone pair in the sp^2-hybridized N is delocalized between double bonds and shows smaller affinity toward CO_2, which makes A3 less effective ligand for CO_2 binding.

Figure 6b shows that the adsorbed amount on A2-BPMO is the highest (i.e., 2.15 mmol/g), that on A1-BPMO is the second (i.e., 0.72 mmol/g), and that on A3-BPMO is the lowest (i.e., 0.40 mmol/g). A2 ligand introduced to BPMO by using TSPED contains the primary and secondary amine groups; however, A1 incorporated to BPMO by using APTES has only one primary amine. A3 has two tertiary amines. As mentioned above, the N lone pairs available in A2-BPMO and A1-BPMO are more accessible toward acidic CO_2 as compared to delocalized N lone pair available in A3-BPMO. Thus, it is evident why the BPMO grafted with A2 ligand has the highest value of CO_2 adsorption.

Another example for amine-containing modifier, which has been frequently studied, is PEI polymer. Figure 7 presents a comparison of CO_2 adsorption on SBA-15- and BPMO-based mesoporous materials measured by using a thermogravimetric analysis (TGA) microbalance at 25 °C and 1 atm. This figure clearly shows the CO_2 adsorption on the PEI-modified SBA-15 and BPMO samples is higher than that on the corresponding unmodified materials. For instance, the PEI/BPMO sample shows higher CO_2 adsorption (1.12 mmol/g) than that obtained for the corresponding BPMO (see Figure 7b).

Also, Figure 7a indicates that the CO_2 adsorption obtained for SBA-15, A2-SBA-15, PEI/SBA-15, and PEI/A2-SBA-15 samples is higher for A2-SBA-15 and PEI/SBA-15 as compared to that of pure SBA-15. Among amine-modified SBA-15-based mesoporous materials, A2-SBA-15 shows the highest CO_2 adsorption up to 1.43 mmol/g. The BET surface area, pore volume, and pore diameter listed in Table 1 for A2-SBA-15 are similar to those of PEI/SBA-15 samples. On the contrary, the CO_2 adsorption on PEI/A2-SBA-15 is lowest (0.17 mmol/g), which is even lower than 0.30 mmol/g of pure SBA-15 (see Table 2).

Figure 7b shows a comparison of the CO_2 adsorption for the BPMO, A2-BPMO, PEI/BPMO, and PEI/A2-BPMO samples. CO_2 adsorption on A2-BPMO and PEI/BPMO is higher as compared to that of pure BPMO. Among amine-modified BPMO-based mesoporous materials, A2-BPMO shows the highest CO_2 adsorption up to 2.15 mmol/g. On the contrary, PEI/A2-BPMO shows the lowest CO_2 adsorption, 0.32 mmol/g, which is even lower than 0.68 mmol/g measured on pure BPMO; this result can be attributed to the pore blocking due to the large amount of modifiers. This small CO_2 uptake can be explained by the very low surface area and small porosity of the double-modified PEI/A2-BPMO sample (Table 1). In addition, the CO_2 uptake by this double-modified sample can be lowered by steric hindrance due to the branched structure of PEI polymer and its high loading inside the pore.

Another important factor is the higher hydrophobicity of the pore walls in the BPMO samples as compared to the SBA-15 samples, which in the former case favors the CO_2 adsorption (see

DOI: 10.1021/acsami.5b00306
ACS Appl. Mater. Interfaces 2015, 7, 6792–6802

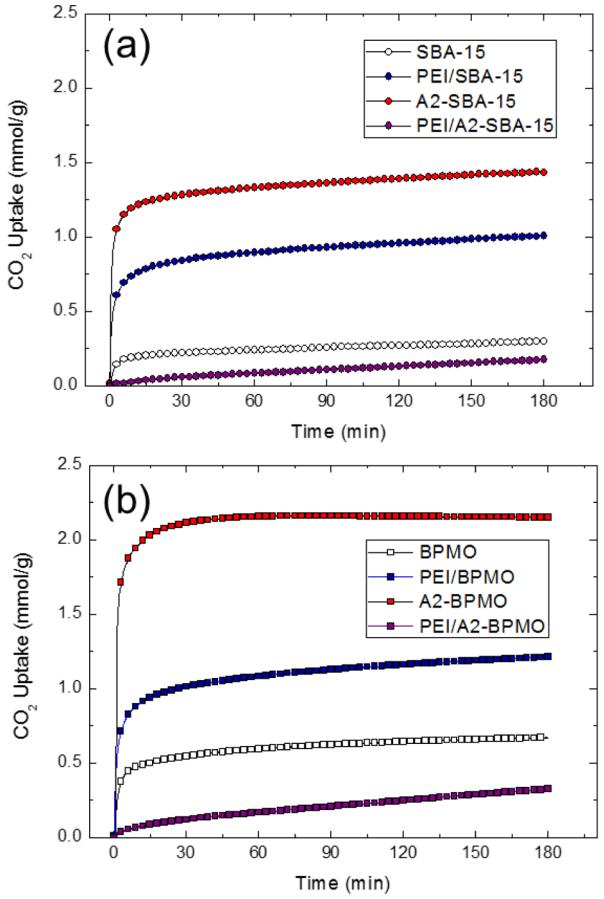

Figure 7. Comparison of CO_2 adsorption kinetics obtained by TGA for (a) SBA-15 and three kinds of PEI/amine-functionalized SBA-15 and (b) BPMO and three kinds of PEI/amine-functionalized BPMO samples.

Figure 7). For instance, the average nitrogen content in the A2-SBA-15 and A2-BPMO samples was determined to be 5.88 and 6.96%, respectively, which correspond to the following concentrations of amine groups: 4.2 and 4.9 mmol/g, respectively. This indicates that the A2-BPMO sample shows higher concentration of amine groups than that evaluated for A2-SBA-15 despite the same experimental conditions used for amine grafting. If one considers the CO_2 volumetric adsorption by the A2-SBA-15 and A2-BPMO samples (Table 2), A2-BPMO shows higher concentration of amine groups by ~17%, but its CO_2 adsorption is 70% higher than that of A2-SBA-15. Also, CO_2 volumetric adsorption can be analyzed by using the ratio of CO_2 molecules/N atom based on the nitrogen content; the values of this ratio are 0.42 and 0.62 for the A2-SBA-15 and A2-BPMO samples, respectively. This result clearly shows that the hydrophobic bridging groups present in the amine-containing siliceous adsorbents favor the CO_2 adsorption. In addition, higher hydrophobicity of the organosiliceous framework in the vicinity of amine groups is beneficial for CO_2 adsorption from gaseous emissions containing small amount of water molecules. Thus, larger concentration of the easily accessible amine groups and higher hydrophobicity of the framework enhance the CO_2 uptake by A2-BPMO as compared to that of A2-SBA-15 (see the CO_2 uptakes in Table 2).

Finally, the effect of post-synthesis modification with PEI on the CO_2 adsorption is briefly discussed. The higher nitrogen loading can be easily achieved in the siliceous materials by PEI modification as compared to those functionalized with A2 amine groups. However, the amine loading is not the only parameter determining the CO_2 uptake. It was shown previously[38,41,42] that the porosity (size and connectivity of pores) of the amine-modified silica-based materials and the steric hindrance caused by highly branched groups affect the CO_2 uptake. The mesopores of SBA-15 and BPMO can be partially or completely blocked during incorporation of PEI polymers, which can make a significant portion of amine groups inaccessible to CO_2 molecules. It was suggested that the lower limit of pore sizes suitable for PEI modification should be above 3.5 nm for efficient CO_2 uptake; modification of smaller pores makes them inaccessible to CO_2 molecules due to the limited diffusion inside pores.[41,42] Branched PEI polymers increase the probability of pore blockage; thus, the PEI-modified A2-SBA-15 and A2-BPMO samples exhibited much lower CO_2 uptakes than those for the corresponding samples without PEI (see Table 2). In addition, the steric hindrance of the PEI segments especially inside the small mesopores decreases the accessibility of amine groups to CO_2 molecules.

Table 2. Carbon Dioxide Uptake Determined from TGA and ASAP Volumetric Sorption Isotherms[a]

	TGA					volumetric adsorption	
			time elapsed for interim adsorption amount (min)				
sample	W_{3h} (mg/g)	C_{3h} (mmol/g)	$t_{80\%}$	$t_{90\%}$	$t_{95\%}$	$W_{1.2\ atm}$ (mg/g)	$C_{1.2\ atm}$ (mmol/g)
SBA-15	13.1	0.30	62.3	112.8	154.8	28.2	0.64
A2-SBA-15	63.0	1.43	6.1	34.6	89.8	78.3	1.78
PEI/SBA-15	40.4	0.92	19.2	69.9	119.0	81.0	1.84
PEI/A2-SBA-15	7.7	0.17	133	155	168	67.8	1.54
BPMO	29.8	0.68	26.3	67.6	111.0	25.2	0.57
A2-BPMO	95.9	2.15	3.1	13.0	52.7	133.3	3.03
PEI/BPMO	49.5	1.12	20.0	64.8	111.0	106.9	2.43
PEI/A2-BPMO	14.3	0.32	129	154	167	51.9	1.18

[a]Notation: W_{3h} = the equilibrium amount of adsorbed CO_2 in mg per gram of the solid after 3 h obtained by TGA; C_{3h} = the equilibrium amount of adsorbed CO_2 in mmoles per gram of the solid after 3 h obtained by TGA; $t_{80\%}$, $t_{90\%}$, $t_{95\%}$ = times elapsed to achieve 80, 90, and 95% of the equilibrium amount of adsorbed CO_2 after 3 h (W_{3h}), respectively; $W_{1.2\ atm}$ = the equilibrium amount of adsorbed CO_2 in mg per gram of the solid measured up to 1.2 atm using ASAP adsorption analyzer; $C_{1.2\ atm}$ = the equilibrium amount of adsorbed CO_2 in mmoles per gram of the solid measured up to 1.2 atm using ASAP volumetric adsorption analyzer.

DOI: 10.1021/acsami.5b00306
ACS Appl. Mater. Interfaces 2015, 7, 6792−6802

The kinetic performance of CO_2 adsorption was compared to the TGA isothermal data plotted as a function of time (Table 2). Most of the TGA kinetic adsorption isotherms show plateau regions and the weights of 80, 90, and 95% as compared to the maximum weights achieved after 3 h; these data were used to estimate how fast the CO_2 uptake reaches the value close to the equilibrium adsorption amount. Data for A2-BPMO show that it takes only 52.7 min to attain 95% of the maximum adsorbed amount, and the second-fastest sample was A2-SBA-15, for which 89.8 min are required to reach the same value. As can be seen from Figure 7, the maximum adsorbed amounts for these two samples are also the highest ones. Therefore, TSPED organosilane (generating A2 amine groups) seems to be the most efficient modifier for preparation of highly efficient adsorbents by taking into account the equilibrium and kinetics aspects of adsorption. Also, the BPMO-based samples showed higher kinetic performance than the SBA-15-based samples, which is attributed to the hydrophobic effect of phenylene groups, having smaller affinity toward water molecules than that of unmodified silica.

Figure 8 shows the pressure-dependent CO_2 adsorption obtained on a volumetric adsorption analyzer. As can be seen from Table 2 and Figure 8, incorporation of a large amount of nitrogen-containing species causes an increase in the CO_2 uptake at 25 °C and 1.2 atm. Note that the CO_2 uptake for SBA-15 is ~0.64 mmol/g, whereas the corresponding capacity of A2-SBA-15 is 1.78 mmol/g. The A2-BPMO sample shows the highest CO_2 capture (up to 3.03 mmol/g) among all samples studied. Usually CO_2 sorption at ambient temperatures is governed through physisorption mechanism. In this case the higher CO_2 uptake is usually obtained for the sample with higher microporosity. In addition to microporosity, this finding indicates the importance of nitrogen species in CO_2 adsorption at room temperature and ambient pressure.

All amine-modified mesoporous samples feature higher CO_2 capture than pure SBA-15 and BPMO samples as shown in Figure 8 and Table 2. It seems that the difference in the adsorption amount between data obtained on the TGA microbalance and ASAP volumetric adsorption analyzer can be attributed to the experimental conditions of pressure-dependent adsorption and TGA measurement at a static atmospheric pressure. Note that the TGA-based microbalance measurement of CO_2 uptake is a dynamic process, whereas ASAP adsorption is an equilibrium one. Moreover, the distance between attached chains containing amine groups can be altered by pressure variation. These differences in the TGA and volumetric adsorption experiments are possible reasons for achieving higher CO_2 uptake on the PEI/A2-SBA-15 and PEI/A2-BPMO when measurements are performed on a volumetric adsorption analyzer.

A small uptake of CO_2 by unmodified SBA-15 silica materials is caused by high hydrophilicity of these materials, which favor adsorption of water molecules. Thus, the presence of small amounts of water in the gas phase can significantly affect the CO_2 uptake of these materials. This effect can be significantly reduced by using, for instance, organosilica instead of silica supports for immobilization of amine groups. In this study we explored the effect of phenylene group in porous siliceous supports on the CO_2 adsorption performance. Therefore, the TEPS-modified BPMO and PEI/TEPS-BPMO samples were studied by using TGA microbalance as shown in Figure 9. Note that TEPS contains also phenylene group, which inevitably increases the affinity of amine-modified materials toward CO_2. The PEI/

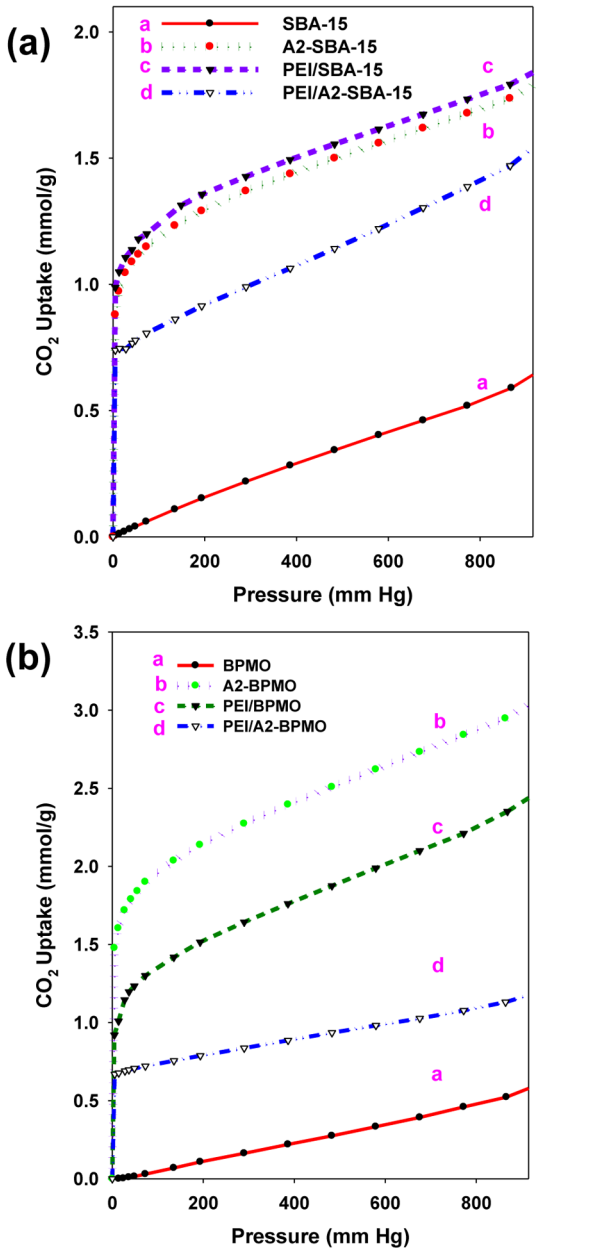

Figure 8. Comparison of pressure-dependent CO_2 adsorption obtained on a volumetric analyzer at 25 °C for (a) SBA-15 and three kinds of PEI/amine-functionalized SBA-15 and (b) BPMO and three kinds of PEI/amine-functionalized BPMO samples.

TEPS-BPMO sample showed slightly higher adsorption performance than PEI/BPMO without TEPS. However, this effect was much less pronounced in the case of the TEPS-modified BPMO sample. It seems that phenylene group itself is not an extraordinary modifier to increase CO_2 adsorption capacity, but it is quite efficient when it is combined with amine groups under appropriate structural environments.

To measure the selectivity for CO_2 adsorption from a gas mixture containing N_2 and CO_2, the A2-BPMO sample was placed on a pan inside cylindrical tube equipped with TGA microbalance in flowing N_2 gas of 40 mL/min and CO_2 gas of 60 mL/min at 25, 80, and 100 °C after being pretreated in flowing N_2 gas of 100 mL/min at 110 °C for 2 h. As shown in Figure 10, the adsorbed amount after 3 h was measured as 1.8 mmol/g at 25 °C, which is ~84% of that for pure CO_2 gas flow of 100 mL/min.

DOI: 10.1021/acsami.5b00306
ACS Appl. Mater. Interfaces 2015, 7, 6792−6802

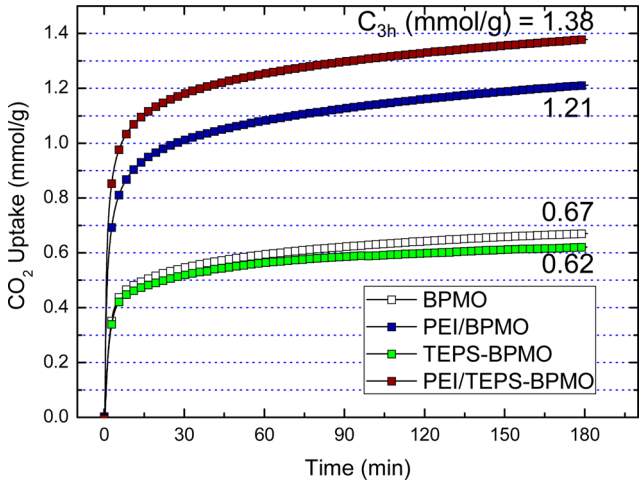

Figure 9. CO_2 adsorption kinetics for phenylene-functionalized BPMO and PEI/phenylene-functionalized BPMO.

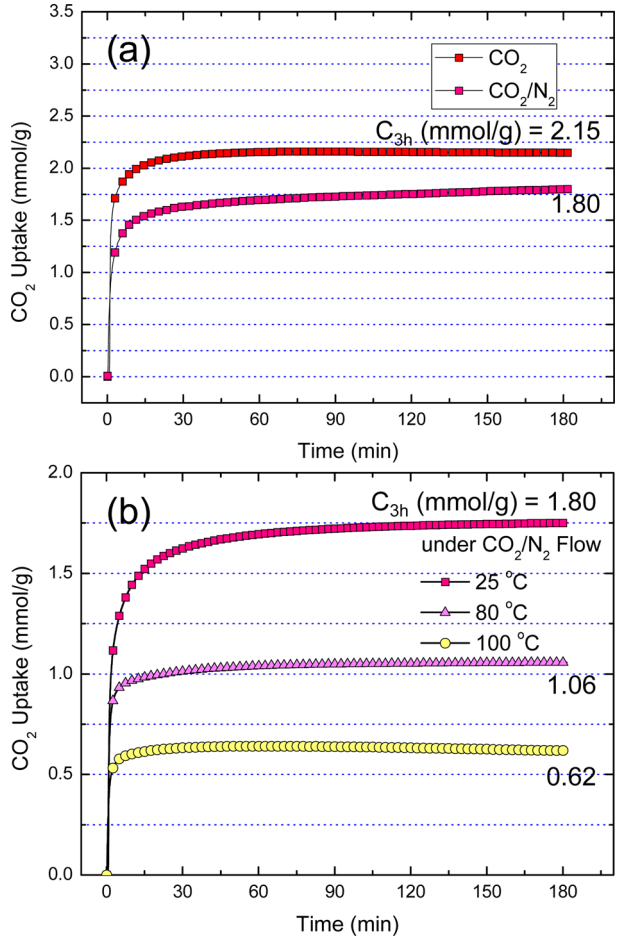

Figure 10. CO_2 adsorption (a) and temperature effect (b) of amine-functionalized BPMO sample under mixed CO_2/N_2 flow.

The adsorbed amounts are reduced more at higher temperatures as shown in Figure 10.

Figure 11 shows the reversibility of the A2-BPMO sample up to nine cycles. The experimental conditions were as those used for selectivity measurements, namely, in flowing N_2 gas of 40 mL/min and CO_2 gas of 60 mL/min at 25 °C after being pretreated in flowing N_2 gas of 100 mL/min at 110 °C for 2 h. At

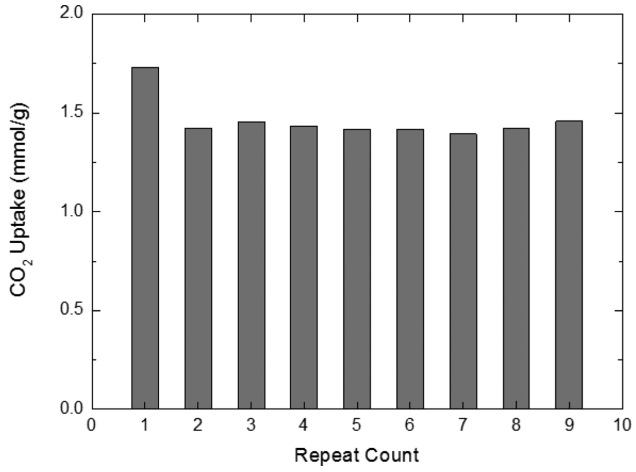

Figure 11. Reversibility test for CO_2 adsorption on the amine-functionalized BPMO sample.

first cycle, the adsorbed amount is slightly reduced to 1.4 mmol/g. However, the nearly constant amounts were obtained repeatedly up to nine cycles

CONCLUSIONS

Mesoporous silica (SBA-15) and BPMO were synthesized in the presence of Pluronic P123 block copolymer template under acidic conditions. SBA-15 and BPMO were functionalized with three kinds of amine-containing organosilanes and PEI polymer. The mesostructure for all amine-modified samples was hexagonal (*p6mm*), and the porosity was varied according to the modification. From solid-state ^{13}C- and ^{29}Si CP-MAS NMR, it was shown that the amine groups exist inside the functionalized mesoporous samples and that the amine-containing chains are chemically linked to both inner and outer surfaces of mesoporous materials. Among several amine-modified SBA-15 and BPMO samples, A2-BPMO showed highest CO_2 uptake up to 2.15 and 3.03 mmol/g, which were obtained on a TGA microbalance and a volumetric adsorption analyzer, respectively. The A2-BPMO sample also showed the fastest adsorption rate; it takes only 13 min to attain 90% of the maximum amount. Selectivity and reproducibility obtained for the A2-BPMO sample show quite good performance in flowing N_2 gas of 40 mL/min and CO_2 gas of 60 mL/min at 25 °C.

In conclusion, the CO_2 uptake of the amine-modified siliceous frameworks depends on the amine structure and loading, available porosity, and hydrophobicity of the aforementioned frameworks. This study shows that the use of organosilica supports for amine immobilization instead of siliceous ones is beneficial for CO_2 adsorption.

ASSOCIATED CONTENT

Supporting Information

Simulated ^{13}C CP-MAS NMR spectra for polyethylene imine and TSPED modifier. This material is available free of charge via the Internet at http://pubs.acs.org.

AUTHOR INFORMATION

Corresponding Authors

*E-mail: echo@seoultech.ac.kr. Phone: +82-2-970-6729. (E.-B.C.)

*E-mail: jaroniec@kent.edu. Phone: +1-330-672-3790. (M.J.)

DOI: 10.1021/acsami.5b00306
ACS Appl. Mater. Interfaces 2015, 7, 6792−6802

Author Contributions

[§]The authors contributed to this work equally.

Notes

The authors declare no competing financial interest.

■ ACKNOWLEDGMENTS

E.-B.C. acknowledges support under the Basic Science Research Program through the National Research Foundation of Korea funded by the Ministry of Education (NRF-2012R1A1A2000855, NRF-2014R1A1A2059947). Experiments at PLS were supported in part by MSIP and POSTECH.

■ REFERENCES

(1) Bachu, S. Sequestration of CO_2 in Geological Media: Criteria and Approach for Site Selection in Response to Climate Change. *Energy Convers. Manage.* **2000**, *41*, 953−970.
(2) Cavenati, S.; Grande, C. A.; Rodrigues, A. E. Adsorption Equilibrium of Methane, Carbon Dioxide, and Nitrogen on Zeolite 13X at High Pressures. *J. Chem. Eng. Data* **2004**, *49*, 1095−1101.
(3) Wang, X. P.; Yu, J. J.; Cheng, J.; Hao, Z. P.; Xu, Z. P. High-Temperature Adsorption of Carbon Dioxide on Mixed Oxides Derived from Hydrotalcite-Like Compounds. *Environ. Sci. Technol.* **2008**, *42*, 614−618.
(4) Caskey, S. R.; Wong-Foy, A. G.; Matzger, A. J. Dramatic Tuning of Carbon Dioxide Uptake via Metal Substitution in a Coordination Polymer with Cylindrical Pores. *J. Am. Chem. Soc.* **2008**, *130*, 10870−10871.
(5) Himeno, S.; Komatsu, T.; Fujita, S. High-Pressure Adsorption Equilibria of Methane and Carbon Dioxide on Several Activated Carbons. *J. Chem. Eng. Data* **2005**, *50*, 369−376.
(6) Huang, H. Y.; Yang, R. T.; Chinn, D.; Munson, C. L. Amine-Grafted MCM-48 and Silica Xerogel as Superior Sorbents for Acidic Gas Removal from Natural Gas. *Ind. Eng. Chem. Res.* **2003**, *42*, 2427−2433.
(7) Harlick, P. J. E.; Sayari, A. Applications of Pore-Expanded Mesoporous Silicas. 3. Triamine Silane Grafting for Enhanced CO_2 Adsorption. *Ind. Eng. Chem. Res.* **2006**, *45*, 3248−3255.
(8) Serna-Guerrero, R.; Da'na, E.; Sayari, A. New Insights into the Interactions of CO_2 with Amine-Functionalized Silica. *Ind. Eng. Chem. Res.* **2008**, *47*, 9406−9412.
(9) Sayari, A.; Belmabkhout, Y. Stabilization of Amine-Containing CO_2 Adsorbents: Dramatic Effect of Water Vapor. *J. Am. Chem. Soc.* **2010**, *132*, 6312−6314.
(10) Yang, J.; Yu, X. H.; Yan, J. Y.; Tu, S. T. CO_2 Capture Using Amine Solution Mixed with Ionic Liquid. *Ind. Eng. Chem. Res.* **2014**, *53*, 2790−2799.
(11) Boot-Handford, M. E.; Abanades, J. C.; Anthony, E. J.; Blunt, M. J.; Brandani, S.; Mac Dowell, N.; Fernández, J. R.; Ferrari, M.-C.; Gross, R.; Hallett, J. P.; Haszeldine, S. R.; Heptonstall, P.; Lyngfelt, A.; Makuch, Z.; Mangano, E.; Porter, R. T. J.; Pourkashanian, M.; Rochelle, G. T.; Shah, N.; Yao, J. G.; Fennell, P. S. Carbon Capture and Storage Update. *Energy Environ. Sci.* **2014**, *7*, 130−189.
(12) Kim, Y. E.; Lim, J. A.; Jeong, S. k.; Yoon, Y. I.; Bae, S. T.; Nam, S. C. Rapid and Ecofriendly Esterification of Alcohols with 2-Acylpyridazinones. *Bull. Korean Chem. Soc.* **2013**, *34*, 3179−3180.
(13) Haszeldine, R. S. Carbon Capture and Storage—How Green Can Black Be. *Science* **2009**, *325*, 1647−1651.
(14) Resnik, K. P. Aqua Ammonia Process for Simultaneous Removal of CO_2, SO_2 and NO_x. *Int. J. Environ. Technol. Manage.* **2004**, *4*, 89−104.
(15) Rezaei, F.; Jones, C. W. Stability of Supported Amine Adsorbents to SO_2 and NO_x in Post Combustion. CO_2 Capture-Single-Component Adsorption. *Ind. Eng. Chem. Res.* **2013**, *52*, 12192−12201.
(16) Sayari, A.; Belmabkhout, Y.; Serna-Guerrero, R. Flue Gas Treatment via CO_2 Adsorption. *Chem. Eng. J.* **2011**, *171*, 760−774.
(17) Xu, X.; Song, C.; Andersen, J. M.; Miller, B. G.; Scaroni, A. W. Novel Polyethylenimine-Modified Mesoporous Molecular Sieve of MCM-41 Type as High-Capacity Adsorbent for CO_2 Capture. *Energy Fuels* **2002**, *16*, 1463−1469.
(18) Xu, X.; Song, C.; Miller, B. G.; Scaroni, A. W. Adsorption Separation of Carbon Dioxide from Flue Gas of Natural Gas-Fired Boiler by a Novel Nanoporous "Molecular Basket" Adsorbent. *Fuel Process. Technol.* **2005**, *86*, 1457−1472.
(19) Franchi, R. S.; Harlick, P. J. E.; Sayari, A. Applications of Pore-Expanded Mesoporous Silica. Development of a High-Capacity, Water-Tolerant Adsorbent for CO_2. *Ind. Eng. Chem. Res.* **2005**, *44*, 8007−8013.
(20) Harlick, P. J. E.; Sayari, A. Applications of Pore-Expanded Mesoporous Silicas. Triamine Silane Grafting for Enhanced CO_2 Adsorption. *Ind. Eng. Chem. Res.* **2006**, *45*, 3248−3255.
(21) Yue, M. B.; Chun, Y.; Cao, Y.; Dong, X.; Zhu, J. H. CO_2 Capture by As-Prepared SBA-15 with an Occluded Organic Template. *Adv. Funct. Mater.* **2006**, *16*, 1717−1722.
(22) Ichikawa, S.; Seki, T.; Tada, M.; Iwasawa, Y.; Ikariya, T. Amorphous Nano-Structured Silicas for High Performance Carbon Dioxide Confinement. *J. Mater. Chem.* **2010**, *20*, 3163−3165.
(23) Liu, S. H.; Wu, C. H.; Lee, H. K.; Liu, S. B. Highly Stable Amine-Modified Mesoporous Silica Materials for Efficient CO_2 Capture. *Top. Catal.* **2010**, *53*, 210−217.
(24) Qi, G. G.; Wang, Y. B.; Estevez, L.; Duan, X. N.; Anako, N.; Pack, A. H.; Li, W.; Jones, C. W.; Giannelis, E. P. High Efficiency Nanocomposite Sorbents for CO_2 Capture Based on Amine-Functionalized Mesoporous Capsules. *Energy Environ. Sci.* **2011**, *4*, 444−452.
(25) Deanna, M. D.; Berend, S.; Jeffrey, R. L. Carbon Dioxide Capture: Prospects for New Materials. *Angew. Chem., Int. Ed.* **2010**, *49*, 6058−6082.
(26) Builes, S.; Vega, L. F. Effect of Immobilized Amines on the Sorption Properties of Solid Materials: Impregnation versus Grafting. *Langmuir* **2013**, *29*, 199−206.
(27) Sayari, A.; Belmabkhout, Y. Stabilization of Amine-Containing CO_2 Adsorbents: Dramatic Effect of Water Vapor. *J. Am. Chem. Soc.* **2010**, *132*, 6312−6314.
(28) Zheng, F.; Tran, D. N.; Busche, B. J.; Fryxell, G. E.; Addleman, R. S.; Zemanian, T. S.; Aardahl, C. L. Ethylenediamine-Modified SBA-15 as Regenerable CO_2 Sorbent. *Ind. Eng. Chem. Res.* **2005**, *44*, 3099−3105.
(29) Knowles, G. P.; Delaney, S. W.; Chaffee, A. L. Diethylenetriamine[propyl(silyl)]-Functionalized (DT) Mesoporous Silicas as CO_2 Adsorbents. *Ind. Eng. Chem. Res.* **2006**, *45*, 2626−2633.
(30) Heydari-Gorji, A.; Belmabkhout, Y.; Sayari, A. Polyethylenimine-Impregnated Mesoporous Silica: Effect of Amine Loading and Surface Alkyl Chains on CO_2 Adsorption. *Langmuir* **2011**, *27*, 12411−12416.
(31) Hoffman, F.; Gulngerich, M.; Klar, P. J.; Froiba, M. Vibrational Spectroscopy of Periodic Mesoporous Organosilicas (PMOs) and Their Precursors: A Closer Look. *J. Phys. Chem. C* **2007**, *111*, 5648−5660.
(32) Cho, E.-B.; Park, J. H.; Jaroniec, M. Structural Stability of Si-C Bonds in Periodic Mesoporous Thiophene- Silicas Prepared under Acidic Conditions. *J. Phys. Chem. C* **2013**, *117*, 21441−21449.
(33) Canck, E. D.; Ascoop, I.; Sayari, A.; Voort, P. V. D. Periodic Mesoporous Organosilicas Functionalized with a Wide Variety of Amines for CO_2 Adsorption. *Phys. Chem. Chem. Phys.* **2013**, *15*, 9792−9799.
(34) Jaroniec, M.; Solovyov, L. A. Improvement of the Kruk−Jaroniec−Sayari Method for Pore Size Analysis of Ordered Silicas with Cylindrical Mesopores. *Langmuir* **2006**, *22*, 6757−6760.
(35) Huh, S.; Wiench, J. W.; Yoo, J.-C.; Pruski, M.; Lin, V. S.-Y. Organic Functionalization and Morphology Control of Mesoporous Silicas via a Co-Condensation Synthesis Method. *Chem. Mater.* **2003**, *15*, 4247−4256.
(36) Caplow, M. Kinetics of Carbamate Formation and Breakdown. *J. Am. Chem. Soc.* **1968**, *90*, 6795−6803.
(37) Sayari, A.; Belmabkhout, Y.; Da'na, E. CO_2 Deactivation of Supported Amines: Does the Nature of Amine Matter. *Langmuir* **2012**, *28*, 4241−4247.
(38) Hiyoshi, N.; Yogo, K.; Yashima, T. Adsorption Characteristics of Carbon Dioxide on Organically Functionalized SBA-15. *Microporous Mesoporous Mater.* **2005**, *84*, 357−365.
(39) Prasetyanto, E. A.; Ansari, M. B.; Min, B. H.; Park, S. E. Melamine Tri-Silsesquioxane Bridged Periodic Mesoporous Organosilica as an

DOI: 10.1021/acsami.5b00306
ACS Appl. Mater. Interfaces 2015, 7, 6792−6802

Efficient Metal-Free Catalyst for CO_2 Activation. *Catal. Today* **2010**, *158*, 252−257.
(40) Dankwerts, P. V. The Reaction of CO_2 with Ethanolamines. *Chem. Eng. Sci.* **1979**, *34*, 443−445.
(41) Zelenak, V.; Halamova, D.; Gaberova, L.; Bloch, E.; Llewellyn, P. Amine-Modified SBA-12 Mesoporous Silica for Carbon Dioxide Capture: Effect of Amine Basicity on Sorption Properties. *Microporous Mesoporous Mater.* **2008**, *116*, 358−364.
(42) Knofel, C.; Descarpentries, J.; Benzaouia, A.; Zelenak, V.; Mornet, S.; Lewellyn, P. L.; Hornebecq, V. Functionalised Micro-/Mesoporous Silica for the Adsorption of Carbon Dioxide. *Microporous Mesoporous Mater.* **2007**, *99*, 79−85.

DOI: 10.1021/acsami.5b00306
ACS Appl. Mater. Interfaces 2015, 7, 6792−6802